17th World Conference on Nondestructive Testing, 25-28 Oct 2008, Shanghai, China

Modeling and analysis of the influence of heating parameters on surface temperature signals

Yingtao LIU [1], Xingwang GUO [2], Guangping GUO [1]

[1] Beijing Institute of Aeronautical Materials, 81#-6 Beijing 100095, China

[2] School of Mechanical Engineering and Automation, Beihang University, Beijing 100083, China

Abstract

To study the influence of heating parameters, including heating pulse duration, heat flux density and heating energy, on surface temperature signals, a 2D model for carbon fiber reinforced plastic sample and a 3D model for aluminum sample were investigated and solved by finite element method (FEM). Calculation results show that the differential temperature between defect and sound areas depends on heating energy, and it gets greater while the heating energy increases. Maximum temperature contrast, differential temperature peak time and best observation time are less sensitive to the change of heat flux density, but affected by heating pulse duration. Maximum temperature contrast is less affected by heating parameters when materials are carbon fiber reinforced plastics (CFRP), so it has more relations to defects and can be used for quantitative analysis of defects. Great heat flux density and short heating pulse is a better choice for detecting defects in metal materials with greater thermal diffusivity, such as aluminum.

Keywords: infrared thermographic nondestructive testing, heating, numerical simulation, finite element method

1. Introduction

Infrared thermographic nondestructive testing (IT NDT) is increasingly used in the inspection of materials and structures due to large surface, rapid and noncontact testing capabilities. Modeling of IT NDT problems allows: 1) exploring relations between surface temperature signals and various parameters such as heating parameters, defect size, specimen size, thermal properties of host material and defect, surface convection and radiation, 2) developing new testing methods and data processing techniques, 3) finding out the best testing method for a given sample and the optimal time to record infrared images.

Studies on modeling and analysis of IT NDT based on 1D, 2D and 3D models, were made using finite difference method (FDM) and FEM[1~2]. Commercial and professional computer programs were already developed. Modeling of complex thermal NDT problems were investigated, such as detection of overlapped defects[3], cracks [4], buried landmines[5], *etc*. In the model of buried landmine detection, the interdependence between surface temperature signals and various complex parameters, such as surface and volumetric moisture, wind speed, the solar radiation, material anisotropy, was demonstrated.

Numerical simulation research was done by Chinese experts based on 1D, 2D and 3D models [6~13]. Models for crack[10] and defects[11] in concrete, and effects of heating intensity[12] and natural convection[13] on surface temperature signals, were studied. But little attention has been paid to the study of influence of heating parameters, including heating pulse duration, heat flux density and heating energy, on surface temperature signals. To study the effect of heating parameters on surface temperature signals, the thermal NDT of carbon fiber reinforced plastics (CFRP) and aluminum are described by 2D and 3D model respectively, and analyzed by FEM in this paper.

2. 2D and 3D Models

The 3D cylindrical model of thermal NDT shown in Fig.1 is used to simulate a delamination in a CFRP specimen. It can be simplified to a 2D model shown in Fig. 2 because it is axisymmetric. In this case a practical defect can be replaced with a disc located at the depth *l*, and the defect radius is r_d, defect thickness *d*. Here *R* and *L* are the radius and thickness of the specimen respectively, and *q* the heat flux density.

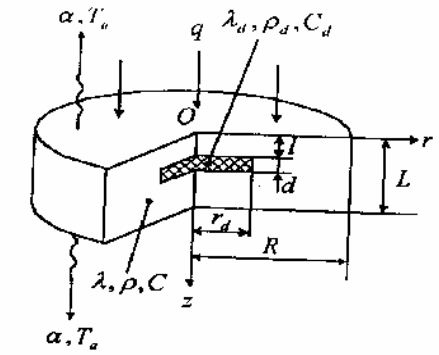

Fig.1. 3D cylindrical model

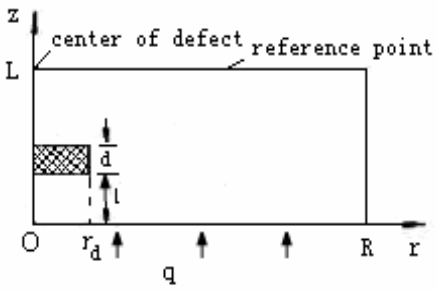

Fig.2. 2D model simplified from 3D cylindrical model

The 3D model shown in Fig. 3 is used to analyze corrosion problems of aluminum. The specimen's size is *B*×*B* and thickness *L*. The corrosion area's size is *b*×*b* and depth *l*.

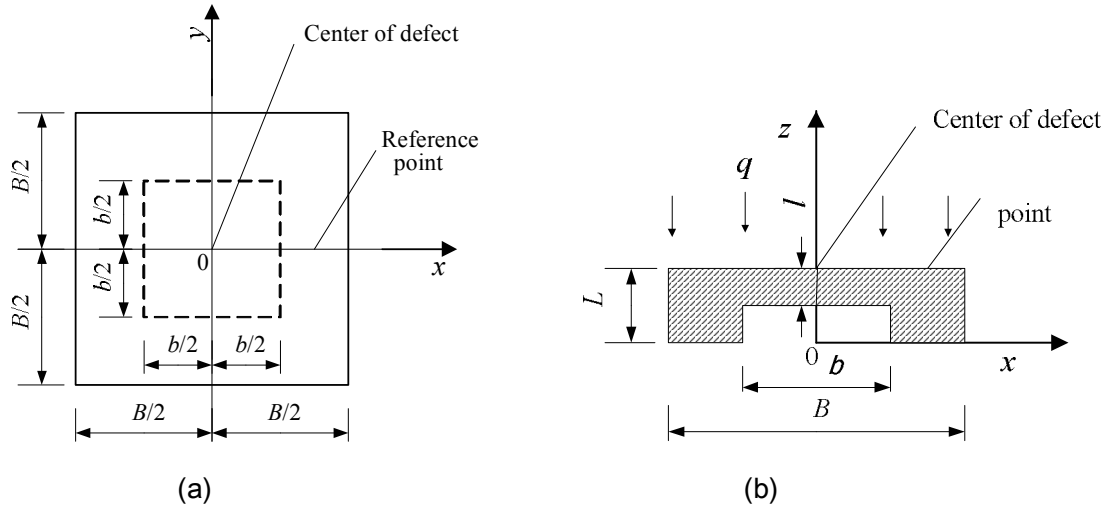

Fig.3. 3D model to analyze corrosion problems. (a)in *xoy* plane (b) in *xoz* plane

Some informative signals are defined as follows:

1. Differential temperature between defect and sound areas ΔT,

$$\Delta T = \theta_d - \theta_{nd} \quad (1)$$

Here

$$\theta_d = T_d - T_0 \quad (2)$$

$$\theta_{nd} = T_{nd} - T_0 \quad (3)$$

T_0, the initial temperature of specimen, T_d, the surface temperature of center point in defect area, T_{nd}, the temperature of reference point.

2. Temperature contrast C,

$$C = \Delta T / \theta_{nd} \quad (4)$$

3. Numerical Simulation

In the 2D model, host material is CFRP and defect material is Teflon. Surfaces of the specimen are supposed to be adiabatic during heating process except heating surface. The initial temperature of specimen is assumed to be the same as ambient temperature. After heating, the boundary condition is convection with the heat transfer coefficient h=10W/(m^2.K). The other parameters for numerical simulation are shown in Table 1, and the thermal properties of materials are shown in Table 2. The results are demonstrated in Table 3, Table 4 and Table 5.

Table 1. Parameters for numerical simulation in 2D model

Specimen thickness L (m)	Defect thickness d (m)	Defect depth l (m)	Specimen radius R (m)	Defect radius r_d (m)
0.003	0.0001	0.001	0.02	0.001

Table 2. Thermal properties of materials

material	Density ρ kg/m^3	Heat capacity c J/(kg·K)	Conductivity λ W/(m·K)	Diffusivity a m^2/s
CFRP[14,15]	1620	760	0.64	5.2×10^{-7}
air(20℃)[16]	1.205	1005	0.0259	2.14×10^{-5}
Teflon[15]	2200	103	0.25	1.1×10^{-6}
aluminum(20℃)[16]	2710	902	236	9.65×10^{-5}

Table 3. Calculation results for analysis of influence of heating flux density on surface temperature signals in 2D model

Group	Heating flux density q_0 (W/ m^2)	Heating pulse duration τ_h (s)	The max. of ΔT ΔT_m(K)	Differential temperature peak time $\tau_m(\Delta T_m)$ (s)	Maximum temperature contrast C_m	Best observation time $\tau_m(C_m)$ (s)
I	0.5×10^6	0.01	0.0895363	1.0726	0.0313028	1.4726

	1.0×10^6	0.01	0.179073	1.0726	0.0313028	1.4726
	1.5×10^6	0.01	0.268609	1.0726	0.0313028	1.4726
II	1.0×10^5	0.1	0.179294	1.1865	0.0313269	1.4865
	1.0×10^6	0.1	1.79294	1.1865	0.0313269	1.4865

In Table 3, when heating pulse duration τ_h was a constant, the maximum of differential temperature between defect and sound areas ΔT_m increased with heating flux density q_0 while maximum temperature contrast C_m, differential temperature peak time $\tau_m(\Delta T_m)$ and best observation time $\tau_m(C_m)$ were not changed.

Table 4. Calculation results for analysis of influence of heating pulse duration on surface temperature signals in 2D model

Heating flux density q_0 (W/ m^2)	Heating pulse duration τ_h (s)	The max. of ΔT ΔT_m(K)	Differential temperature peak time $\tau_m(\Delta T_m)$ (s)	Maximum temperature contrast C_m	Best observation time $\tau_m(C_m)$ (s)
1.0×10^6	0.01	0.179073	1.0726	0.0313028	1.4726
1.0×10^6	0.015	0.268635	1.0736	0.0313048	1.4736
1.0×10^6	0.02	0.358110	1.1478	0.0313294	1.4478
1.0×10^6	0.1	1.79294	1.1865	0.0313269	1.4865

In Table 4, when q_0 was a constant, ΔT_m and $\tau_m(\Delta T_m)$ increased with τ_h while C_m and $\tau_m(C_m)$ were changed a little.

Table 5. Calculation results when heating energy was a constant in 2D model

Group	Heating flux density q_0 (W/ m^2)	Heating pulse duration τ_h (s)	The max. of ΔT ΔT_m(K)	Differential temperature peak time $\tau_m(\Delta T_m)$ (s)	Maximum temperature contrast C_m	Best observation time $\tau_m(C_m)$ (s)
I	1.0×10^6	0.01	0.179073	1.0726	0.0313028	1.4726
	1.0×10^5	0.1	0.179294	1.1865	0.0313269	1.4865
II	1.5×10^6	0.01	0.268609	1.0726	0.0313028	1.4726
	1.0×10^6	0.015	0.268635	1.0736	0.0313048	1.4736

In Table 5, when heating energy was a constant, ΔT_m and C_m were changed little, but $\tau_m(\Delta T_m)$ and $\tau_m(C_m)$ were changed with τ_h.

In the 3D model, specimen material is aluminum. Surfaces of the specimen are supposed to be adiabatic during heating process except heating surface. The initial temperature of specimen is assumed to be the same as ambient temperature. After heating, the boundary condition is h_1=10W/(m^2.K) on sound furface, and h_2=5W/(m^2.K) on defect surface. The other parameters for numerical simulation are shown in Table 6 and the results are demonstrated in Table 7, Table 8 and Table 9.

Table 6. Parameters for numerical simulation in 3D model

Specimen size B (m)	Specimen thickness L (m)	Defect size b (m)	Defect depth l (m)
0.01	0.002	0.002	0.0018

Table 7. Calculation results for analysis of influence of heating flux density on surface temperature signals in 3D model

Group	Heating flux density q_0 (W/ m^2)	Heating pulse duration τ_h (s)	The max. of ΔT ΔT_m(K)	Differential temperature peak time $\tau_m(\Delta T_m)$ (s)	Maximum temperature contrast C_m	Best observation time $\tau_m(C_m)$ (s)
I	1.0×10^5	0.01	0.00299921	0.021480	0.0132676	0.021480
	1.0×10^6	0.01	0.0323840	0.019373	0.0146370	0.021471
	1.0×10^7	0.01	0.323840	0.019373	0.0146370	0.021471
II	1.0×10^6	0.05	0.0890891	0.053978	0.00814864	0.055912
	2.0×10^6	0.05	0.178178	0.053978	0.00814864	0.055912

In Table 7, when τ_h was a constant, ΔT_m increased with q_0 while C_m, $\tau_m(\Delta T_m)$ and $\tau_m(C_m)$ were changed little.

Table 8. Calculation results for analysis of influence of heating pulse duration on surface temperature signals in 3D model

Heating flux density q_0 (W/ m^2)	Heating pulse duration τ_h (s)	The max. of ΔT ΔT_m(K)	Differential temperature peak time $\tau_m(\Delta T_m)$ (s)	Maximum temperature contrast C_m	Best observation time $\tau_m(C_m)$ (s)
1.0×10^6	0.01	0.0323840	0.019373	0.0146370	0.021471
1.0×10^6	0.05	0.0890891	0.053978	0.00814864	0.055912
1.0×10^6	0.1	0.100285	0.10236	0.00724801	0.034317

In Table 8, when q_0 was a constant, ΔT_m and $\tau_m(\Delta T_m)$ increased with τ_h while C_m decreased. It is demonstrated that ΔT_m and C_m could not reach their maximum at the same τ_h if only changing τ_h. $\tau_m(C_m)$ firstly increased and then decreased because two extreme points emerged on the C-time evolution curve, and their relative magnitude also changed with the increase of τ_h (in Fig. 4). The C-time evolution curve has a sharp shape when τ_h is short, and this ease the determination of $\tau_m(C_m)$ and the quantitative analysis of defects.

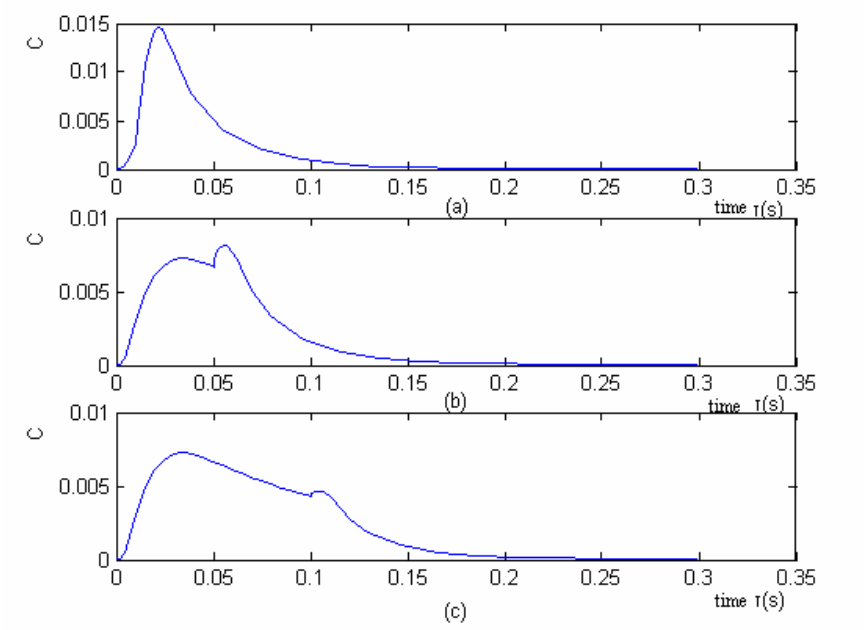

Fig.4. Influence of heating pulse durationτ_h on temperature contrast C in 3D model

$q_0 = 1.0\times10^6$ W/ m^2 (a) τ_h =0.01s , (b) τ_h =0.05s , (c) τ_h =0.1s

Table 9. Calculation results when heating energy was a constant in 3D model

Heating flux density q_0 (W/ m^2)	Heating pulse duration τ_h (s)	The max. of ΔT ΔT_m(K)	Differential temperature peak time $\tau_m(\Delta T_m)$ (s)	Maximum temperature contrast C_m	Best observation time $\tau_m(C_m)$ (s)
1.0×10^7	0.01	0.323840	0.019373	0.0146370	0.021471
2.0×10^6	0.05	0.178178	0.053978	0.00814864	0.055912
1.0×10^6	0.1	0.100285	0.10236	0.00724801	0.034317

In Table 9, when heating energy was a constant, ΔT_m and C_m increased with q_0. This is different from the above results of 2D because of the difference of thermal properties of CFRP and aluminum, so great heat flux density and short heating pulse is a better choice for detecting defects in aluminum.

4. Conclusion

From the numerical simulation results of 2D and 3D models, conclusions are made as follows:

(1) The differential temperature between defect and sound areas depends on heating energy, and it gets greater while the heating energy increases.

(2) Maximum temperature contrast C_m, differential temperature peak time τ_m (ΔT_m) and best observation time $\tau_m(C_m)$ are less sensitive to the change of heat flux density, but affected by heating pulse duration.

(3) Maximum temperature contrast C_m is less affected by heating parameters when materials are carbon fiber reinforced plastics (CFRP), so it has more relations with defect

characteristics and can be used in quantitative analysis of defects.

(4) Great heat flux density and short heating pulse is a better choice for detecting defects in metal materials with greater thermal diffusivity, such as aluminum.

References

[1] U. Galietti, S. Ladisa, C. Pappalettere, L. Spagnolo. Hybrid procedure to characterize hidden defects in composite.
Thermosense XXIV. SPIE, 2002, Vol.4710. P599-609

[2] Vladimir P. Vavilov. Accuracy of thermal NDE numerical simulation and reference signal evolutions.
Thermosense-XXI. SPIE, 1999, Vol.3700. P14-19

[3] Vladimir P. Vavilov. Three-dimensional analysis of transient thermal NDT problems by data simulation and processing.
Thermosense XXII. SPIE, 2000, Vol.4020. P152-163

[4] Robin Steinberger, Thomas Grünberger, Paul O'Leary. Simulations and analytical models for optimization of photothermal surface crack detection.
Thermosense XXIII. SPIE, 2001, Vol.4360. P524-533

[5] Vladimir P.Vavilov, Douglas Burleigh, Alexey G.Klimov. Advanced modeling of thermal NDT problems: from buried landmines to defects in composites.
Thermosense XXIV. PIE, 2002, Vol.4710. P507-521

[6] Wang Yanwu, Yang Li, Sun Fengri. Numerical simulation research of infrared nondestructive testing on the resistive and capacitive defects inside material.
Laser & Infrared, 2006, Vol.36, No.8. P657-660

[7] Xiao Jinsong, Yan Tianpeng. Computer simulation of the U-tube ground heat exchanger for GSHP.
Journal of Beijing university of technology, 2006, Vol.32, No.1. P48-52

[8] Zhao Shibin, Zhao Jia, Zhang Cunlin, Ding Youfu, Li Yanhong. Finite element simulation and analysis for type identification of defects under material surfaces in infrared thermal wave nondestructive detection.
Journal of Applied Optic, 2007, Vol.28, No.5. P559-563

[9] Li Dapeng, Yang Zhidong, Sun Fengrui. Application of finite element method in the infrared non-destructive testing with single surface heating.
Mechanical & Electrical Engineering Magazine, 2005, Vol.22, No.2. P24-29

[10] Li Dapeng, Zhang Liqun, Zhao Yansong. Research of Character Pick-up and Graph Reconstruction of Crack in Infrared Non-destructive Testing.
Computer Measurement & Control, 2005, Vol.13, No.7. P624-626

[11] Huang Hongmei, Wei Zhen. 3-D Finite Element Method Simulation of Infrared Non- destructive Testing.
J. of Anhui University of Technology, 2006, Vol.23, No.3. P313-314

[12] Li Guohua, Zhao Huiyou, Zhu Hongxiu, Qu Jingxin, Wu Lixin. Numerical optimum of non-destructive testing by infrared thermography. 2004

[13] Fan Chunli, Sun Fengrui, Yang Li. Temperature distribution of defect surface and effect of natural convection on thermographic inspection.
Laser & Infrared, 2005, Vol.35, No.7. P504-507

[14] Sergio Marinetti, Alberto Muscio, Paolo Giulio Bison, Ermanno Grinzato. Modeling of thermal non-destructive evaluation techniques for composite materials. In: Ralph B. Dinwiddie, Dennis H. Le Mieux.
Thermosense XXII. Bellingham: SPIE, 2000, Vol.4020. P164-173

[15]Bison P G, Bressan C, Cavaccini G, *et al*. NDE of composite materials by Thermal method and Shearography.
In: Wurzbach R N, Burleigh D D. Proc SPIE Thermosense-XIX. Bellingham: SPIE, 1997, Vol.3056. P220-229
[16]Yang Shiming, Tao Wenquan. Heat transfer. 3th Edition.
Beijing: Higher Education Press,1998. P420-424